EAST EUROPEAN JOURNAL OF PHYSICS. 1. 162-172 (2023)
DOI:10.26565/2312-4334-2023-1-20 ISSN 2312-4334

THE GREEN SYNTHESIS OF COPPER OXIDE NANOPARTICLES USING THE MORINGA OLEIFERA PLANT AND ITS SUBSEQUENT CHARACTERIZATION FOR USE IN ENERGY STORAGE APPLICATIONS[†]

Imosobomeh L. Ikhioya[a]*, Edwin U. Onoh[a], Agnes C. Nkele[a,e], Bonaventure C. Abor[a], B.C.N. Obitte[a], M. Maaza[b,c,d], Fabian I. Ezema[a,b,c,d]

[a]Department of Physics and Astronomy, University of Nigeria, Nsukka, 410001, Enugu State, Nigeria
[b]Nanosciences African Network (NANOAFNET) iThemba LABS-National Research Foundation, 1 Old Faure Road, Somerset West 7129, P.O. Box 722, Somerset West, Western Cape Province, South Africa
[c]UNESCO-UNISA Africa Chair in Nanosciences/Nanotechnology, College of Graduate Studies, University of South Africa (UNISA), Muckleneuk Ridge, P.O. Box 392, Pretoria, South Africa
[d]Africa Centre of Excellence for Sustainable Power and Energy Development (ACE-SPED), University of Nigeria, Nsukka, Nigeria
[e]Department of Physics, Colorado State University, Fort Collins, U.S.A.
**Corresponding Author e-mail: imosobomeh.ikhioya@unn.edu.ng*
Received December 7, 2022; revised February 1, 2023; accepted February 2, 2023

Research Highlights:

- Successful synthesis of CuO NPs using extracts from dried, finely ground Moringa Oleifera as the reducing/capping agent
- The green synthesize CuO NPs displayed supercapacitive behavior.
- The reflection spectra demonstrate that the material exhibits low reflectance properties in the medium ultraviolet region.
- Good absorbance and low band gap energy values (E_g = 2.5 eV).
- Potential application to supercapacitor and other energy storage

In this study, we describe the environmentally friendly synthesis of copper oxide (CuO) and its subsequent characterization for use in supercapacitors. Using extracts from dried, finely ground Moringa Oleifera as the reducing/capping agent, we created the CuO NP. The produced NPs were then examined using X-ray Diffractometer (XRD), Ultraviolet-Visible spectroscopy, energy dispersive spectroscopy (EDS), and scanning electron microscopy (SEM). Electrochemical analysis techniques like cyclic voltammetry (CV) and electrochemical impedance spectroscopy (EIS) review were utilized to look at the electrochemical behavior of CuO-based electrodes. The analysis that followed determined that the green synthesize CuO NPs displayed supercapacitive behavior. This suggests that the synthesized CuO NPs will naturally encourage application as supercapacitive electrodes because it has been found that NPs absorbance varies linearly with NPs concentration, the 0.6 moles of CuO NPs produced the highest absorbance reading of 0.35 at 398 nm. The reflection spectra demonstrate that the material exhibits low reflectance properties in the medium ultraviolet region. However, as the spectra move toward the visible light region, the reflectance rises to its maximum value of 16 percent in the short ultraviolet region. The calculated crystallite sizes are as follows: 0.2 mols CuO NP, 0.3 mols CuO NP, 0.4 mols CuO NP, 0.5 mols CuO NP, and 0.6 mols CuO NP at 43.14 nm, 43.68 nm, 24.23 nm, 5.70 nm, and 12.87 nm, respectively, where Average D = 25.93 nm is the average crystalline size across all samples. the emergence of cubic grains that resemble nanorods with tube-like holes, SEM images demonstrate that CuO NPs can be distinguished from one another as seen in 0.2 mole CuO NPs.

Keywords: *CuO NPs; Supercapacitors; Energy storage; Moringa oleifera; Cyclic voltammetry*
PACS: 81.07.Wx, 82.47.Uv, 84.60.Ve, 43.30.Ky, 29.20.D

1. INTRODUCTION

The growing interest in electrochemical energy storage technologies, in particular fuel cells, super-capacitors, and batteries, promising to displacing the non-renewable systems of energy storage devices currently in vogue, is a direct result of the rising demand for renewable and environmentally friendly supply of energy and energy storage devices. Supercapacitors, one of the energy storage technologies currently in use, have been found to offer higher power and energy density than secondary batteries and conventional capacitors, respectively [1, 2]. These characteristics make them acceptable and advantageous for use in array of industries, from electronic consumer products to hybrid electrified vehicles [3].

Due to their rich redox chemical valences for use in pseudo-capacitive batteries, transition metals, and metallic oxides have drawn significant attention in the search for materials with good potential for electrochemical energy storage devices. Copper oxides have been regarded as the most alluring among these metallic oxides over time because of their numerous, established uses, such as in the fields of catalysis, gas sensors, anti-fungal/anti-microbial research, and batteries [4]. Overall, it is favorable and preferable due to its enticingly high capacitance, brilliant electrochemical performance, environmentally friendly nature, and affordable raw material costs [5-7].

According to its two valences, copper exists naturally in two oxide forms: cupric or copper II oxide (CuO) and cuprous or copper (II) oxide (CuO). Several methods have reportedly been used to prepare CuO and Cu_2O electrodes for supercapacitors [8–12]. Various CuO nanostructures, including nanorods, nanoflakes, nanowires, nanospheres,

[†] ***Cite as:*** I.L. Ikhioya, E.U. Onoh, A.C. Nkele, B.C. Abor, B.C.N. Obitte, M. Maaza, and F.I. Ezema, East Eur. J. Phys. **1**, 162 (2023), https://doi.org/10.26565/2312-4334-2023-1-20

nanoplatelets, nanoribbons, nanoflowers, micro-roses, micro-wool, flowers, willow-leaves, and dandelion-like CuO microspheres, have also been prepared using these various techniques [13–25].These nanostructures, as well as other properties like particle/grain size, superficial zone, aperture volume, and lucidity, which are governed by the strategy of deposition and specifications in particular pH, concentration of precursor materials, temperature etc., are extremely important for the electrochemical functioning of CuO-based electrodes as well as other electrode materials [26–28].

In this study, we present findings regarding the structure and characteristics of CuO NPs produced from Moringa oleifera using a green synthesis method. CuO NPs are produced using conventional methods as well, but studies have shown that green synthesis techniques are more effective at producing NPs that are low cost, adept at being characterized, and less likely to fail [29]. The use of plant extracts, fungi, bacteria, and yeast as reductants, capping, and reinforcing agents during the fabrication of the nanoparticles emphasizes the green synthesis method of producing metal oxide NPs, which ultimately strengthens biocompatibility and widespread production [30,31]. The great diversity of plants allows for the possibility of obtaining variations in nanoparticle size, shape, and morphology for a wide range of applications, production cost and time, and the presence of metabolites substances like polyphenols, phenolic acids, sugars, proteins, terpenoids and alkaloids which contribute to the bio-reduction and stabilization of the metal ions into nanoparticles make plant extracts the most promising of all these different types. [32-34]

Solvents, stabilizing or capping agents, and reducing agents are the three factors that are typically taken into account and studied when thinking about green synthesis methods. [35]. The green synthesis method is primarily regarded as environmentally friendly because it uses water or ethanol to dissolve the metal-ion precursors instead of organic solvents that might leave toxic residues behind after the synthesis process. Furthermore, since research has demonstrated that biomolecules can function as capping and reducing agents, the use of some complex chemicals that were previously employed to convert metallic salts to pure metals has been eliminated. [36]

The Moringa oleifera, is a very quickly growing, drought-resistant tree that is indigenous to India [37]. It is a member of the moringacea family. Researchers have become interested in moringa Oleifera primarily because it is a rich source of striking, potent phytochemicals. The Moringa Oleifera has demonstrated great potential in several applications, including medicine, biodiesel production, water purification, and food production, due to the presence of these phytochemicals, which include vitamins, natural sugars, alkaloids, minerals, organic acids, phenolic acids, phytosterols and flavonoids [38].

Even though few studies are already reported on the use of extracts from Moringa oleifera leaf acting as efficient reducing as well as capping agents for the biosynthesis of copper nanoparticles, for this study we investigated for the first time the uses of these nanoparticles produced using this method in supercapacitors and electrochemical energy storage devices.

CuO nanoparticles were produced and examined using a novel sol-gel process by Aparna Y, et al. They found that these particles could be used as superconductors, monitors, storage devices, and solar power transmission. Due to their cleanliness, lack of impurities, and well-organized shape, copper oxide nanoparticles make excellent catalysts for chemical reactions [45].

Due to the fascinating dimension-dependent chemical and physical properties of CuO in comparison to micrometer-sized particles, nanostructured materials provide a versatile range that can be used in a variety of situations [46]. Researchers have used bacteria like Streptococcus pyogenes, Pseudomonas aeruginosa, E. coli, and Staphylococcus aureus to examine the antibacterial properties of copper nanoparticles. The highest inhibition zone was discovered when they used the disk diffusion tests of nanoparticles dispersed in mycelial growth to investigate the bactericidal effects of copper nanoparticles. Escherichia coli and Staphylococcus aureus were both inhibited by copper nanoparticles, with inhibitory activities of 14 mm and 10 mm, respectively, in E. coli and Staphylococcus aureus. It was found that the type of nanoparticle can affect how susceptible bacteria are to it.

Gold and silver nanoparticles are now used in the printing of responsive global frameworks, according to Deng D, et al [47]. Copper nanoparticles are a substitute as a result of their modest cost and excellent electro conductivity. Notwithstanding, a significant obstacle in their use as conductive inks is the spontaneous oxidation of copper nanoparticles. According to the paper, the antioxidative copper composites were simply mixed with a lactonic acid ethanol solution before being deposited on glass slides. It has been proven that lactonic acid can react with nearby copper oxides so as to give rise to copper carboxylate, and eventually reduced by heating with nitrogen at a temperature of 200°C to copper. Due to CuO's intriguing characteristics, SF Shaffiey and his colleagues synthesized it and assessed its bactericidal abilities. CuO, a transition metal oxide, is among the most crucial. It is used in many different technological applications, including photosensitive devices, gas sensors, and critical temperature superconductors, to name a few. It has recently been looked into as an antibacterial agent for various bacteria. The process depends on the straightforward interaction of copper sulfate and de-ionized water, which is devoid of dangerous solvents, organics, and amines. Its bactericidal activity was evaluated against Aeromonas hydrophila ATCC 7966T bacteria. CuO nanoparticles have a great deal of potential as an antibacterial agent against A. hydrophila, claims this study [48].

The supercapacitive properties of CuO-based electrodes were explored via electrochemical impedance spectroscopy (EIS), cyclic voltammetry (CV) and galvanostatic charge-discharge (GCD).

2. EXPERIMENTAL DETAILS

50 g of ground air-dried Moringa oleifera leaves were immersed in 500 ml of distilled water and heated between 60 and 700°C. After allowing the extracts to cool at room temperature, they were filtered twice with filter paper (Whatman No.1 filter paper).

30 ml of the extracts were added to the $CuSO_4 \cdot 5H_2O$ solution after 1.59 g of $CuSO_4 \cdot 5H_2O$ was added to 50 ml of water and vigorously stirred until a solution was formed. When extracts are added, the solution's color abruptly changes from the copper salt solution's pale blue to dark green precipitates, which may be an indication that nanoparticles have formed. The solution was heated until it formed a brown paste, which was then transferred to a crucible and dried at 100°C for an hour before being annealed at 400°C for two hours. The powder, which was a darkish brown color, was then kept and used in subsequent research. The process was repeated for the following amounts of CuO NPs: 2.39 g, 3.19 g, 3.99 g, and 4.78 g, which correspond to 0.3 mols, 0.4 mols, 0.5 moles, and 0.6 moles, respectively.

While structural analyses were accomplished by utilizing an X-ray diffractometer, the surface morphology of the respective formed CuO NPs was investigated using the image obtained from scanning electron microscopy (SEM) (XRD). Measurements were made using the CuO-based electrode which is the working electrode, platinum as the counter electrodes, while the Ag/AgCl electrode is the reference electrode in 1M KOH electrolyte so as to scrutinize the supercapacitor rendition of the CuO NPs.

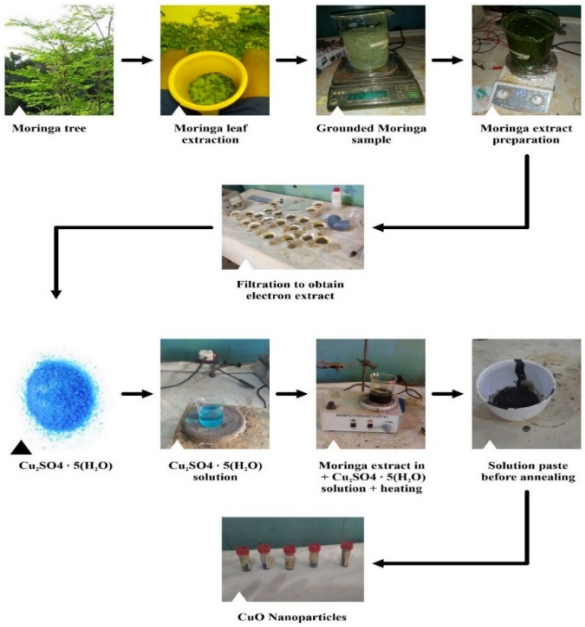

Figure 1. Pictorial diagram of the experimental Procedure

3. RESULTS AND DISCUSSIONS

3.1. XRD analysis

Figure 2 displays the copper oxide nanoparticles' XRD pattern. The pattern showed diffraction peaks at 34.9°, 43.3°, 50.5°, and 74.1°, respectively, which corresponded to reflections from planes; (222), (110), (200), and (311). The inter-atomic distance between the atoms and the crystallite size of the CuO NPs were determined through analysis.

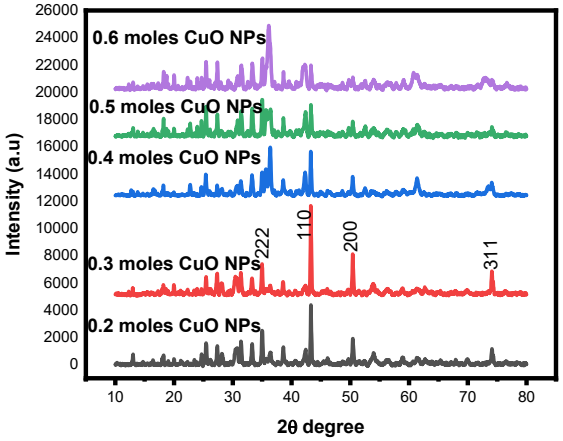

Figure 2. X-Ray Diffraction partner of the synthesized CuO NPs

The crystallite size D (nm) was calculated from the XRD data by employing the Debye Scherrer formula [39]:

$$D = \frac{K\lambda}{\beta cos(\theta)} \quad (1)$$

where K is the Scherrer constant, which ranges from 0.68 to 2.08, and D is the crystallite size. Its value has been determined to be 0.94 for spherical crystallites with cubic symmetry. Where $CuK\alpha$= 1.5406 Å is the X-ray wavelength, $\boldsymbol{\beta}$ connoting line broadening about FWHM measured in radians, while $\boldsymbol{\theta}$ in degrees connotes Bragg's angle.

The calculated crystallite sizes are 0.2 mols CuO NP, 0.3 mols CuO NP, 0.4 mols CuO NP, 0.5 mols CuO NP, and 0.6 mols CuO NP, respectively, at 43.14 nm, 43.68 nm, 24.23 nm, 5.70 nm, and 12.87 nm, where Average D = 25.93 nm is the average crystalline size across all the samples.The interplanar spacing was also obtained using Bragg's Law given as:

$$\boldsymbol{d_{hkl} = \frac{n\lambda}{2\theta};} \tag{2}$$

The Scherrer's constant remains unchanged, and n stands for the number of fringes. After combining all the data for different peak values, the interatomic spacing's mean value was determined to be 3.7755 Å.

3.2. SEM analysis

The surface morphologies of the synthesized CuO NPs at various concentrations were thoroughly examined using SEM images. The initial stages in the formation of the microstructure include nucleation, a surface heterogeneous reaction, particle accumulation, followed by organizing itself to much larger particles. The development of nanorod-like grains with cubic shapes and tube-like holes, as was seen in 0.2 mole CuO NPs, distinguishes CuO NPs across the board, according to the SEM images. A strong candidate for use in supercapacitors, this morphology also suggests high porosity and offers a reactive surface that is helpful for ion transport. [40]

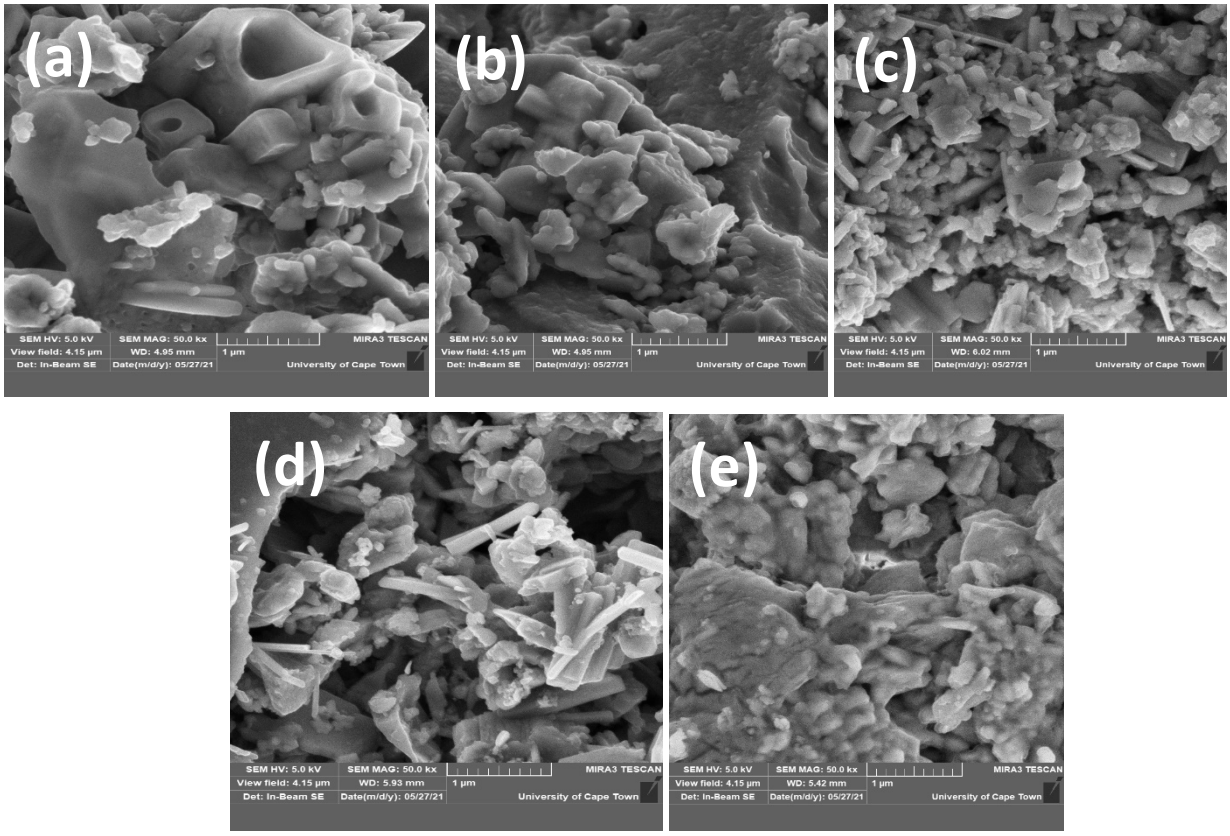

Figure 3. SEM images of the synthesized CuO NPs for 0.2 mols, 0.3 mols, 0.4 mols, 0.5 mols, and 0.6 mols corresponding to a, b, c, d, and e respectively.

3.3. EDS analysis

In order to ascertain the elemental configuration of the examined CuO NPs, an EDS method is used. EDS analysis revealed the presence of Cu and also revealed the presence of S, suggesting that the precursor was a bluestone (CuSO4)

3.4. Optical analysis of the synthesized CuO NPs

UV spectroscopy was used to obtain the optical studies of the various sample concentrations, which are listed as 0.2 mols, 0.3 mols, 0.4 mols, 0.5 mols, and 0.6 mols. These studies are discussed further below. A plot of absorbance versus wavelength in Figure 5 (a) demonstrates that the 0.2 moles of CuO NPs absorb very little in the short-wavelength ultraviolet region, with a minimum value of 0.0635 at 328 nm. Finally, the NPs' absorbance gradually increased until it reached a maximum value of 0.183 at 384 nm in the medium ultraviolet region. The 0.6 moles of CuO NPs produced the

highest absorbance reading of 0.35 at 398 nm because it is observed that NPs absorbance varies linearly with NPs concentration. However, this is in agreement with the theoretical predictions of the Beer-Lambert law, which states that the amount of absorption is proportional to the concentration of the absorber. In general, it is significant to note that this material's low absorbance properties, as compared to lithium-ion batteries, make it a good choice for use in supercapacitors as energy storage devices and in the pursuit of environmentally friendly forms of energy supply. Figure 5 (b), The transmittance spectra convey that the absorbance spectra have an inverse relationship. The NPs with the highest concentration, 0.6 mol, corresponds to the lowest percentage transmittance in Figure 5 (b), while the NPs' absorbance value is at its highest. The 0.2 mols CuO NPs, on the other hand, exhibit greater radiation transmission in the short-wavelength ultraviolet region, as shown in Figure 5 (b). Eventually getting to its maximum, of 86.5 percent at 323 nm. This percentage transmittance value slightly drops to a minimum percentage value of 66 percent at 390 nm. The samples' high transmittance characteristics in the visible light and short-wavelength ultraviolet regions demonstrate their suitability for both passive and active solar technology. Figure 5 (c), The material has low reflectance characteristics in the medium ultraviolet region, as shown by the reflection spectra. The reflectance, however, increases to its maximum value of 16 percent in the short ultraviolent region as the spectra moves toward the visible light region. In the region of visible light, a continuous spectrum is seen as the spectra slightly decreases from the maximum to about 15%.

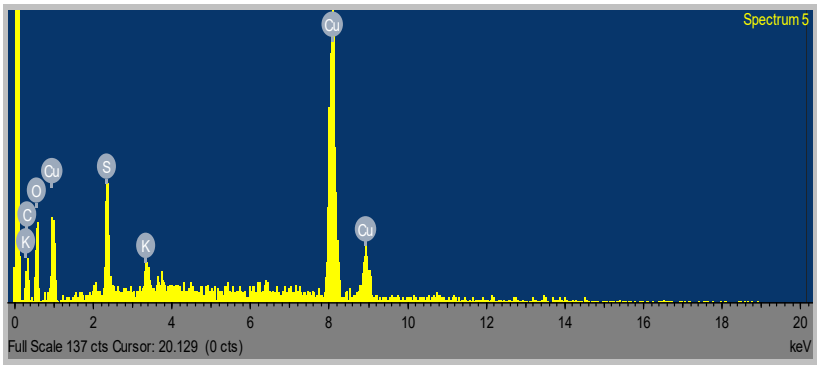

Figure 4. EDS spectrum of the synthesized CuO NPs

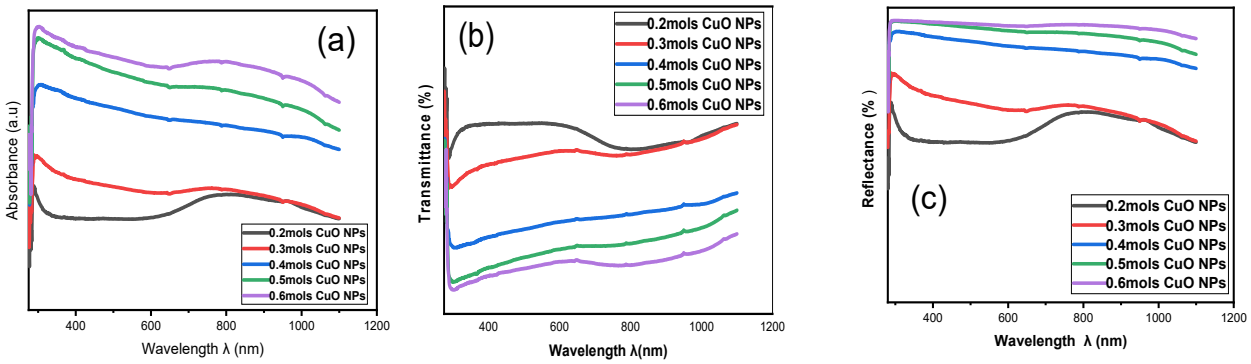

Figure 5. Spectra of (a) Absorbance, (b) transmittance, and (c) reflectance of the synthesized CuO NPs

The distance between an electron's valence band and conduction band is depicted in Figure 6(a), and this distance is known as the band gap or energy gap.

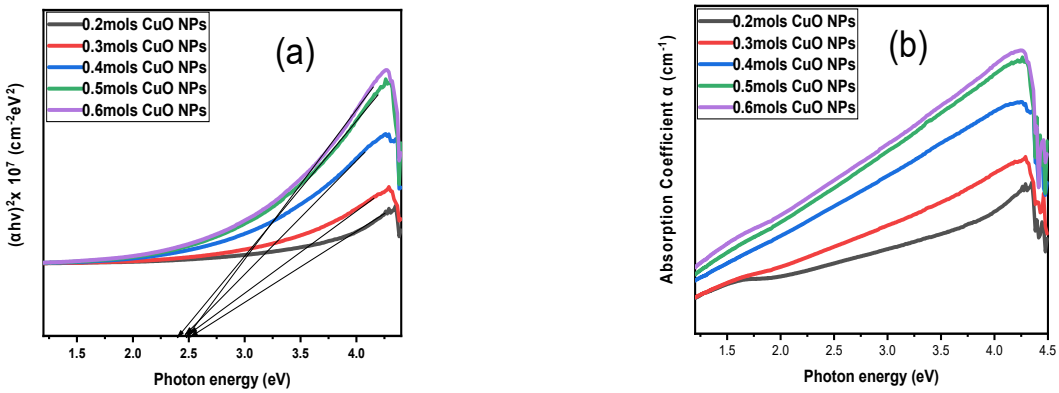

Figure 6. Spectra of (a) Absorption coefficient square and (b) absorption coefficient of the synthesized CuO NPs

An important factor in determining a material's electrical conductivity is the energy band gap, outlining an energy range where electronic state cannot exist. If the atom's valence band is filled and the conduction band is extremely empty, electrons cannot move through the material. On the contrast, if there is electron transfer from the valence to the conduction band, current can flow [19]. The average band gap of the CuO NPs across all samples, as seen in the Tauc plot in Figure 6 (a), was 2.5 eV. All of the prepared samples have a high light absorption coefficient in the ultraviolet and visible light region, indicating an increase in the likelihood of direct transitions occurring, as shown in Figure 6 (b), which is the plot of absorption coefficient against photon energy. Additionally, it was observed that the absorption coefficient gradually rises as photon energy rises, which is related to the interactions between the incident electrons and the electrons in the CuO NPs.

The atoms of the medium continuously absorb and re-emit light particles as it passes through it, slowing down the light's speed over time. Since refractive index and wavelength are inversely proportional, light moves more slowly as the refractive index increases. According to the theoretical prediction, the refractive index gradually decreases as the photon energy increases as seen in the spectra. In Figure 7 (a) the maximum refractive index for the 0.2 mol CuO NPs was reached; however, this value slightly decreased as the photon energy of the incident radiation increased toward the visible light and near-infrared regions. The extinction coefficient is a measurement of how strongly a substance absorbs light at any given fixed wavelength. It measures how electromagnetic waves are dampened when they enter a medium. The following formula relates the extinction coefficient to the absorption coefficient:

$$\boldsymbol{K = \frac{\lambda \alpha}{4\pi}} \tag{3}$$

The maximum extinction coefficient for all samples of CuO NPs was found at E = 4.32 eV in the ultraviolent region according to Figure 7(b), with a proportional increase as sample concentration increased. The optical conductivity of the CuO NPs reveals that the optical conductivity of the CuO NPs increases as the photon energy increases as seen in Figure 7 (c).

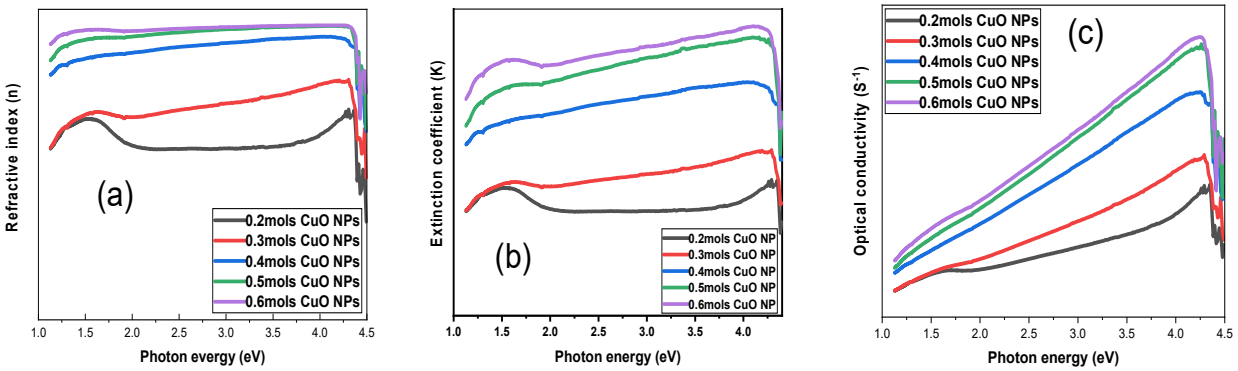

Figure 7. Spectra of (a) Refractive index, (b) extinction coefficient, and (c) optical conductivity of the synthesized CuO NPs

The imaginary component of the dielectric constant describes a material's capacity to permanently absorb energy from a time-varying electric field, while the real component describes a material's capacity to interact with an electric field (store and remit energy) without doing so. This suggests that a high imaginary part dielectric constant absorbs a lot of energy.

The Dielectric constant and refractive index of the material is related via the equation;

$$\boldsymbol{\varepsilon = n^2} \tag{5}$$

The maxima and minima of the electromagnetic radiation spectrum occur in the same energy region when the real dielectric against photon energy and the imaginary dielectric constant plots are compared.

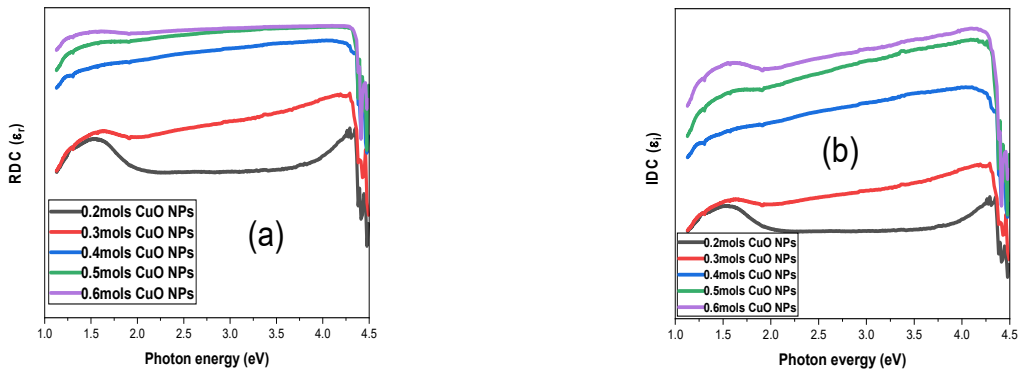

Figure 8. Spectra of (a) real dielectric constant and (b) imaginary dielectric constant of the synthesized CuO NPs

The maximum value was obtained for the 0.2 mols CuO NPs in the ultraviolet region at ε_r and ε_i equivalent to 5.58 and 0.0687, respectively, at the same value for Photo energy equal to 4.42 eV. Moving forward, it was also noted that a direct relationship existed between the two terms of the dielectric constant and the sample concentration, with the 0.6 mol CuO NPs sample providing the highest values of ε_r and ε_I of 6.98 and 0.1504 respectively at the same photon energy, which in this case decreased slightly to 4.25 eV.

3.5. Electrochemical impedance spectroscopy studies (EIS)

An EIS study was conducted to scrutinize the interrelation between the surface electronic properties of the electrolyte (1M KOH) and the CuO-based NPs electrodes, and also to verify their diverse reaction kinetics and resistances. The EIS measurements were assessed using frequency ranges from 1.0 Hz – 100.0 kHz.0.2 mols CuO-based NPs and 0.3 moles CuO-based NPs electrodes have unvarying electrolytic resistance (Re) together with working electrode's resistance (Rw) respectively as 13.0 Ω and 0.9 Ω, 0.4 mols CuO-based NPs and 0.5 moles CuO-based NPs electrodes have unvarying electrolytic resistance (Re) as the working electrode's resistance (Rw) of 12.0 Ω and 0.8 Ω, respectively, while 0.6mols of CuO NPs have its electrolytic resistance (Re) as 12.0 Ω whereas its working electrode's resistance (Rw) is 0.7Ω. This suggests that the CuO-based NPs electrodes offer great interfacial area.

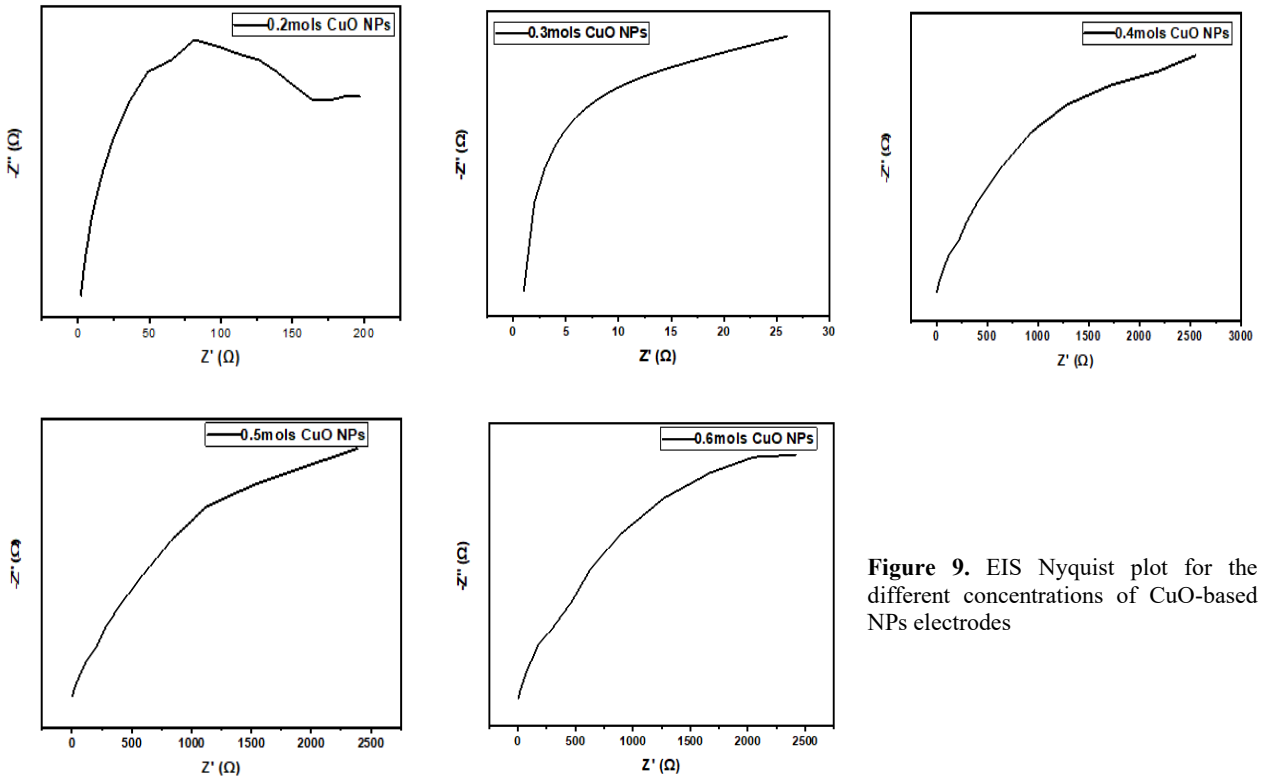

Figure 9. EIS Nyquist plot for the different concentrations of CuO-based NPs electrodes

3.6. Cyclic voltammetry (CV)

The utilization of a cyclic voltammetry was to understand capacitive behavior exhibited by the electrode which is a result of the convenience of the CuO-based NPs electrode to the 1M KOH electrolyte. The different concentrations of the CuO-based NPs electrodes were recorded at the same scan rate of 10 mV/s.

From the plot, the very sharp peaks of the CV curves are due to redox reactions occurring during the process which is consistent with the Cu^{2+} to Cu^{+} reduction process and Cu^{+} to Cu^{2+} oxidation process [45]. From our CV curve, the specific capacitance of the different concentrations of CuO-based electrodes was all calculated using this equation [41-44];

$$C_s = \frac{\int IdV}{mS\Delta V} \tag{6}$$

Given that $\int IdV$ is gotten by incorporating the area under the CV curve, where specific capacitance is connoted as Cs, the current is given as I, voltage as V, the scan rate is given as S, and M as the active mass of the different concentrations of the CuO NPs electrode. The specific capacitance of the different CuO NPs gave 176 Fg^{-1} for 0.2 mols CuO NP, 181 Fg^{-1} for 0.3 mols, 322 Fg^{-1} for 0.4mols, 328 Fg^{-1} for 0.5mols and 212 Fg^{-1} for 0.6 mols. The high specific capacitance that is gotten could be credited to the rapid transportation of charges during intercalation between the CuO NPs electrode and the 1M KOH electrolyte.

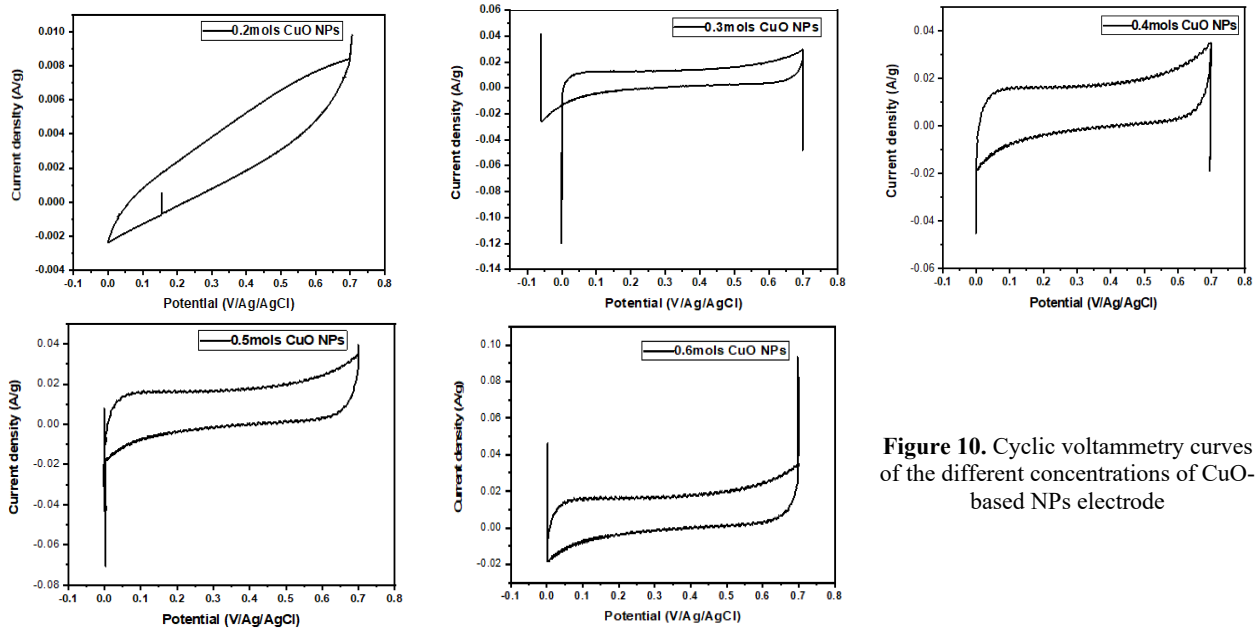

Figure 10. Cyclic voltammetry curves of the different concentrations of CuO-based NPs electrode

3.7. Galvanostatic charge discharge (GCD)

We also conducted the galvanostatic charge-discharge (GCD) estimation in an unchanged electrolyte environment with the CV. From the GCD curves, it could be observed that the material exhibits pseudo-capacitive performance. From the GCD, the specific capacitance was calculated using this equation [41-44];

$$C_s = \frac{It_d}{m\Delta V} \tag{7}$$

Given that the specific capacitance is connoted as Cs, the current is given as I, while the time of discharge is given as td. For the denominator, m is the active mass of the CuO-based electrode given as m, while the voltage is given as V.

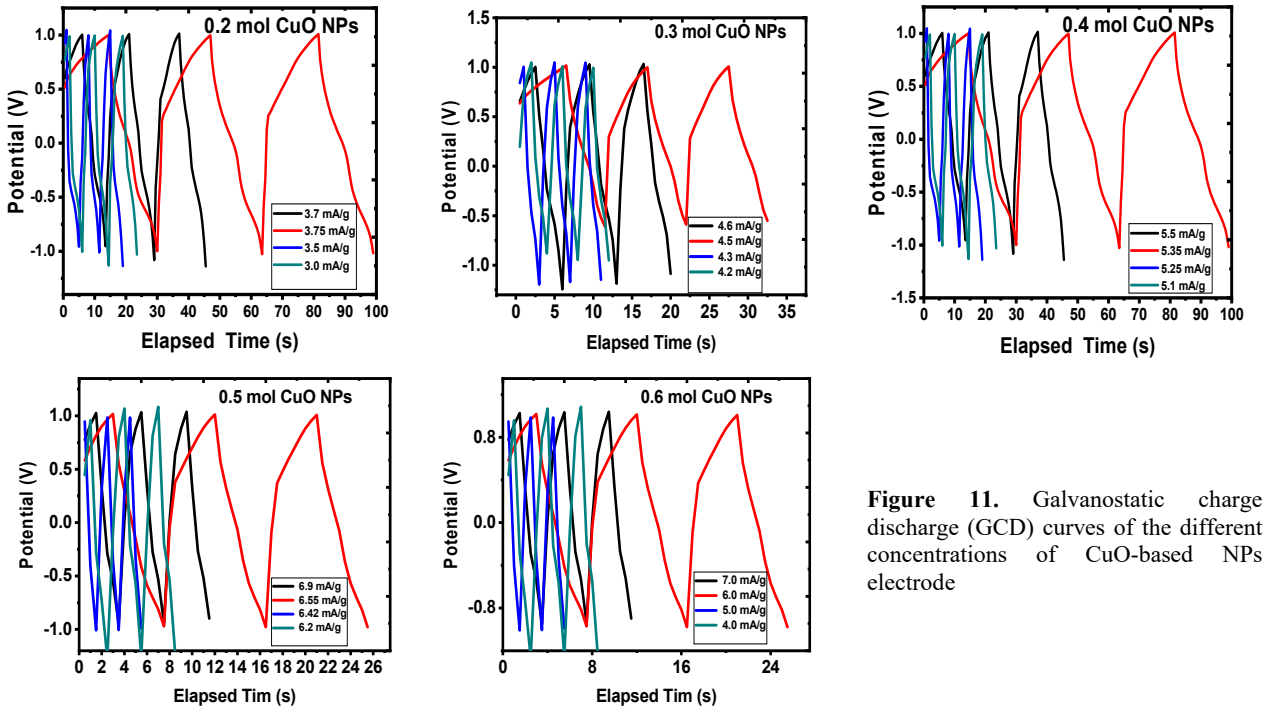

Figure 11. Galvanostatic charge discharge (GCD) curves of the different concentrations of CuO-based NPs electrode

4. CONCLUSION

In conclusion, due to the rising interest and demand for supercapacitors as energy storage devices when compared to lithium-ion batteries and the quest for an environmentally friendly form of energy supply, we successfully synthesized CuO NPs using an environmentally friendly, cost-effective, and simple approach; which is green synthesis as against the conventional chemical methods used. The low band gap values of 2.5 eV and the resultant electrochemical analysis test

results carried out on the different samples establish the fact that the synthesized CuO NPs exhibited supercapacitive properties, hence can be used in supercapacitor and other energy storage applications.

Funding. The authors received no funding for this research.

Conflicts of Interest. None to declare

Ethical Statement. The paper reflects the authors' research and analysis truthfully and completely.

Data Availability Statement. The data that support the findings of this study are available on request from the corresponding author.

Author contribution. The study's conceptualization, methodology, and experiments were all contributed to by all of the writers. Imosobomeh L. Ikhioya, Edwin U. Onoh, Bonaventure C. Abor, B.C.N. Obitte, and Agnes C. Nkele did the material preparation, methodology, experiment, graph plotting, and analysis. Imosobomeh L. Ikhioya and Edwin U. Onoh wrote the manuscript's first draft, with the help of Malik Maaza and Fabian I. Ezema for editing. The final manuscript was read and approved by all writers.

ORCID IDs

Imosobomeh L. Ikhioya, https://orcid.org/0000-0002-5959-4427

REFERENCES

[1] M. Heon, S. Lofland, J. Applegate, R. Nolte, E. Cortes, J.D. Hettinger, P.L. Taberna, P. Simon, P. Huang, M. Brunet, and Y. Gogotsi, "Continuous carbide-derived carbon films with high volumetric capacitance", Energy & Environmental Science, **4**(1), 135-138D (2011). https://doi.org/10.1039/c0ee00404a

[2] D. Ahn, I. Yoo, Y.M. Koo, N. Shin, J. Kim, and T.J. Shin, "Effects of cobalt-intercalation and polyaniline coating on electrochemical performance of layered manganese oxides", Journal of Materials Chemistry, **21**(14), 5282-5289 (2011). https://doi.org/10.1039/C0JM03548C

[3] G. Wee, W.F. Mak, N. Phonthammachai, A. Kiebele, M.V. Reddy, B.V.R. Chowdari, G. Gruner, M. Srinivasan, and S.G. Mhaisalkar, "Particle size effect of silver nanoparticles decorated single walled carbon nanotube electrode for supercapacitors", Journal of the Electrochemical Society, **157**(2), A179 (2009). https://doi.org/10.1149/1.3267874

[4] J. Liu, J. Wang, C. Xu, H. Jiang, C. Li, L. Zhang, J. Lin, and Z.X. Shen, "Advanced energy storage devices: basic principles, analytical methods, and rational materials design", Advanced science, **5**(1), 1700322 (2018). https://doi.org/10.1002/advs.201700322

[5] H. Zhang, and M. Zhang, "Synthesis of CuO nanocrystalline and their application as electrode materials for capacitors", Materials Chemistry and Physics, **108**(2-3), 184-187 (2008). https://doi.org/10.1016/j.matchemphys.2007.10.005

[6] V.D. Patake, S.S. Joshi, C.D. Lokhande, and O.S. Joo, "Electrodeposited porous and amorphous copper oxide film for application in supercapacitor", Materials Chemistry and Physics, **114**(1), 6-9 (2009). https://doi.org/10.1016/j.matchemphys.2008.09.031

[7] X. Zhang, W. Shi, J. Zhu, D.J. Kharistal, W. Zhao, B.S. Lalia, H.H. Hng, and Q. Yan, "High-power and high-energy-density flexible pseudocapacitor electrodes made from porous CuO nanobelts and single-walled carbon nanotubes", ACS nano, **5**(3), 2013-2019 (2011). https://doi.org/10.1021/nn1030719

[8] I.M. Tiginyanu, O. Lupan, V.V. Ursaki, L. Chow, and M. Enachi, "3-11 - Nanostructures of metal oxides", Comprehensive Semiconductor Science and Technology, **3**, 396-479 (2011). https://doi.org/10.1016/B978-0-44-453153-7.00105-X

[9] S.E. Moosavifard, M.F. El-Kady, M.S. Rahmanifar, R.B. Kaner, and M.F. Mousavi, "Designing 3D highly ordered nanoporous CuO electrodes for high-performance asymmetric supercapacitors", ACS applied materials & interfaces, **7**(8), 4851-4860 (2015). https://doi.org/10.1021/am508816t

[10] W. Xu, S. Dai, G. Liu, Y. Xi, C. Hu, and X. Wang, "CuO nanoflowers growing on carbon fiber fabric for flexible high-performance supercapacitors", Electrochimica Acta, **203**, 1-8 (2016). https://doi.org/10.1016/j.electacta.2016.03.170

[11] D.P. Dubal, G.S. Gund, R. Holze, H.S. Jadhav, C.D. Lokhande, and C.J. Park, "Surfactant-assisted morphological tuning of hierarchical CuO thin films for electrochemical supercapacitors", Dalton Transactions, **42**(18), 6459-6467 (2013). https://doi.org/10.1039/C3DT50275A

[12] S.K. Shinde, D.P. Dubal, G.S. Ghodake, D.Y. Kim, and V.J. Fulari, "Nanoflower-like CuO/Cu (OH) 2 hybrid thin films: Synthesis and electrochemical supercapacitive properties", Journal of Electroanalytical Chemistry, **732**, 80-85 (2014). https://doi.org/10.1016/j.jelechem.2014.09.004

[13] G. Fan, and F. Li, "Effect of sodium borohydride on growth process of controlled flower-like nanostructured Cu2O/CuO films and their hydrophobic property", Chemical engineering journal, **167**(1), 388-396 (2011). https://doi.org/10.1016/j.cej.2010.12.090

[14] H. Li, S. Yu, and X. Han, "Fabrication of CuO hierarchical flower-like structures with biomimetic superamphiphobic, self-cleaning and corrosion resistance properties", Chemical Engineering Journal, **283**, 1443-1454 (2016). https://doi.org/10.1016/j.cej.2015.08.112

[15] Y. Ma, H. Li, R. Wang, H. Wang, W. Lv, and S. Ji, "Ultrathin willow-like CuO nanoflakes as an efficient catalyst for electro-oxidation of hydrazine", Journal of Power Sources, **289**, 22-25 (2015). https://doi.org/10.1016/j.jpowsour.2015.04.151

[16] Y. Ma, H. Wang, J. Key, S. Ji, W. Lv, and R. Wang, "Control of CuO nanocrystal morphology from ultrathin "willow-leaf" to "flower-shaped" for increased hydrazine oxidation activity", Journal of Power Sources, **300**, 344-350 (2015). https://doi.org/10.1016/j.jpowsour.2015.09.087

[17] D.P. Dubal, G.S. Gund, R. Holze, and C.D. Lokhande, "Mild chemical strategy to grow micro-roses and micro-woolen like arranged CuO nanosheets for high performance supercapacitors", Journal of Power Sources, **242**, 687-698 (2013). https://doi.org/10.1016/j.jpowsour.2013.05.013

[18] G. Wang, J. Huang, S. Chen, Y. Gao, and D. Cao, "Preparation and supercapacitance of CuO nanosheet arrays grown on nickel foam", Journal of Power Sources, **196**(13), 5756-5760 (2011). https://doi.org/10.1016/j.jpowsour.2011.02.049

[19] A.C. Nwanya, D. Obi, K.I. Ozoemena, R.U. Osuji, C. Awada, A. Ruediger, M. Maaza, F. Rosei, and F.I. Ezema, "Facile synthesis of nanosheet-like CuO film and its potential application as a high-performance pseudocapacitor electrode", Electrochimica Acta, **198**, 220-230 (2016). https://doi.org/10.1016/j.electacta.2016.03.064
[20] W. Zhang, H. Wang, Y. Zhang, Z. Yang, Q. Wang, J. Xia, and X. Yang, "Facile microemulsion synthesis of porous CuO nanosphere film and its application in lithium-ion batteries", Electrochimica Acta, **113**, 63-68 (2013). https://doi.org/10.1016/j.electacta.2013.09.043
[21] J. Wang, and W.D. Zhang, "Fabrication of CuO nanoplatelets for highly sensitive enzyme-free determination of glucose", Electrochimica Acta, **56**(22), 7510-7516 (2011). https://doi.org/10.1016/j.electacta.2011.06.102
[22] F. Cao, X.H. Xia, G.X. Pan, J. Chen, and Y.J. Zhang, "Construction of carbon nanoflakes shell on CuO nanowires core as enhanced core/shell arrays anode of lithium ion batteries", Electrochimica Acta, **178**, 574-579 (2015). https://doi.org/10.1016/j.electacta.2015.08.055
[23] B. Heng, C. Qing, D. Sun, B. Wang, H. Wang, and Y. Tang, "Rapid synthesis of CuO nanoribbons and nanoflowers from the same reaction system, and a comparison of their supercapacitor performance", RSC advances, **3**(36), 15719-15726 (2013). https://doi.org/10.1039/C3RA42869A
[24] Z. Zhang, H. Che, Y. Wang, L. Song, Z. Zhong, and F. Su, "Preparation of hierarchical dandelion-like CuO microspheres with enhanced catalytic performance for dimethyldichlorosilane synthesis", Catalysis Science & Technology, **2**(9), 1953-1960 (2012). https://doi.org/10.1039/C2CY20199B
[25] M.J. Deng, C.C. Wang, P.J. Ho, C.M. Lin, J.M. Chen, and K.T. Lu, "Facile electrochemical synthesis of 3D nano-architectured CuO electrodes for high-performance supercapacitors", Journal of Materials Chemistry A, **2**(32), 12857-12865 (2014). https://doi.org/10.1039/C4TA02444C
[26] A. Vlad, N. Singh, J. Rolland, S. Melinte, P.M. Ajayan, and J.F. Gohy, "Hybrid supercapacitor-battery materials for fast electrochemical charge storage", Scientific reports, **4**, 4315 (2014). https://doi.org/10.1038/srep04315
[27] G. Wang, L. Zhang, and J. Zhang, "A review of electrode materials for electrochemical supercapacitors", Chemical Society Reviews, **41**(2), 797-828 (2012). https://doi.org/10.1039/C1CS15060J
[28] X. Zhang, W. Shi, J. Zhu, D.J. Kharistal, W. Zhao, B.S. Lalia, H.H. Hng, and Q. Yan, "High-power and high-energy-density flexible pseudocapacitor electrodes made from porous CuO nanobelts and single-walled carbon nanotubes", ACS nano, **5**(3), 2013-2019 (2011). https://doi.org/10.1021/nn1030719
[29] T.M. Abdelghany, A.M. Al-Rajhi, M.A. Al Abboud, M.M. Alawlaqi, A. GanashMagdah, E.A. Helmy, and A.S. Mabrouk, "Recent advances in green synthesis of silver nanoparticles and their applications: about future directions. A review", BioNanoScience, **8**(1), 5-16 (2018). https://doi.org/10.1007/S12668-017-0413-3
[30] M. Nasrollahzadeh, F. Ghorbannezhad, Z. Issaabadi, and S.M. Sajadi, "Recent developments in the biosynthesis of Cu-based recyclable nanocatalysts using plant extracts and their application in the chemical reactions", The Chemical Record, **19**(2-3), 601-643 (2019). https://doi.org/10.1002/tcr.201800069
[31] M. Nasrollahzadeh, S. Mahmoudi-GomYek, N. Motahharifar, and M.G. Gorab, "Recent developments in the plant-mediated green synthesis of Ag-based nanoparticles for environmental and catalytic applications", The Chemical Record, **19**(12), 2436-2479 (2019). https://doi.org/10.1002/tcr.201800202
[32] M. Nasrollahzadeh, M. Atarod, M. Sajjadi, S.M. Sajadi, and Z. Issaabadi, "Plant-mediated green synthesis of nanostructures: mechanisms, characterization, and applications", in: *Interface science and technology,* Vol. 28, (Elsevier, Amsterdam, 2019). pp. 199-322.
[33] M. Shah, D. Fawcett, and S. Sharma, S.K. Tripathy and G.E.J. Poinern, "Green Synthesis of Metallic Nanoparticles via Biological Entities", Materials (Basel), **8**(11), 7278–7308 (2015). https://doi.org/10.3390%2Fma8115377
[34] V.V. Gusel'nikova, and D. Korzhevskiy, "NeuN as a neuronal nuclear antigen and neuron differentiation marker", Acta Naturae, **7**(2), 42-47 (2015). https://pubmed.ncbi.nlm.nih.gov/26085943
[35] C.P. Devatha, and A.K. Thalla, "Green synthesis of nanomaterials", Synthesis of inorganic nanomaterials, 169-184 (2018). https://doi.org/10.1016/B978-0-08-101975-7.00007-5
[36] H. Duan, D. Wang, and Y. Li, "Green chemistry for nanoparticle synthesis", Chemical Society Reviews, **44**(16), 5778-5792 (2015). https://doi.org/10.1039/C4CS00363B
[37] L. Gopalakrishnan, K. Doriya, and D.S. Kumar, "Moringa oleifera: A review on nutritive importance and its medicinal application", Food science and human wellness, **5**(2), 49-56 (2016). https://doi.org/10.1016/j.fshw.2016.04.001
[38] R.K. Saini, I. Sivanesan, and Y.S. Keum, "Phytochemicals of Moringa oleifera: a review of their nutritional, therapeutic and industrial significance", Biotech, **6**(2), 1-14 (2016). https://doi.org/10.1007/s13205-016-0526-3
[39] P. Scherrer, "Bestimmungdergrosse und der innerenstruktur yon kolloiteilchenmittels", Gott. Nachr Math. Phys, **2**, 98-100 (1918).
[40] S.K. Shindea, M.B. Jalak, G.S. Ghodake, N.C. Maile, V.S. Kumbhar, D.S. Lee, V.J. Fulari, and D.-Y. Kim, "Chemically synthesized nanoflakes-like NiCo2S4 electrodes for high-performance supercapacitor application", Appl. Surf. Sci. **466**, 822-829 (2019). https://doi.org/10.1016/j.apsusc.2018.10.100
[41] H.E. Nsude, K.U. Nsude, G.M. Whyte, R.M. Obodo, C. Iroegbu, M. Maaza, and F.I. Ezema, "Green synthesis of $CuFeS_2$ nanoparticles using mimosa leaves extract for photocatalysis and supercapacitor applications", Journal of Nanoparticle Research, **22**(11), 1-13 (2020). https://doi.org/10.1007/s11051-020-05071-7
[42] S. Najib, F. Bakan, N. Abdullayeva, R. Bahariqushchi, S. Kasap, G. Franzò, et al, "Tailoring morphology to control defect structures in ZnO electrodes for high-performance supercapacitor devices", Nanoscale, **12**(30), 16162-16172 (2020). https://doi.org/10.1039/D0NR03921G
[43] M.Ö. Alaş, A. Güngör, R. Genç, and E. Erdem, "Feeling the power: robust supercapacitors from nanostructured conductive polymers fostered with Mn 2+ and carbon dots", Nanoscale, **11**(27), 12804-12816 (2019). https://doi.org/10.1039/C9NR03544C
[44] M. Toufani, S. Kasap, A. Tufani, F. Bakan, S. Weber, and E. Erdem, "Synergy of nano-ZnO and 3D-graphene foam electrodes for asymmetric supercapacitor devices", Nanoscale, **12**(24), 12790-12800 (2020). https://doi.org/10.1039/D0NR02028A
[45] A.O. Aliyu, S. Garba, and O. Bognet, "Green Synthesis, Characterization and Antimicrobial Activity of Vanadium Nanoparticles Using Leaf Extract of Moringa Oleifera," **11**(1), 42–48 (2018). https://doi.org/10.9790/5736-1101014248

[46] A.A. Radhakrishnan, and B.B. Beena, "Structural and Optical Absorption Analysis of CuO Nanoparticles", Indian Journal of Advances in Chemical Science, **2**(2), 158–161 (2014). https://www.ijacskros.com/artcles/IJACS-M64.pdf
[47] D. Deng, T. Qi, Y. Chen, Y. Jin, and F. Xiao, "Preparation of antioxidative nano copper pastes for printed electronics application," in: *13th International Conference on Electronic Packaging Technology & High Density Packaging*, (2012). pp. 250-253. https://doi.org/10.1109/ICEPT-HDP.2012.6474611
[48] S.F. Shaffiey, M. Shapoori, A. Bozorgnia, and M. Ahmadi, "Synthesis and evaluation of bactericidal properties of CuO nanoparticles against Aeromonas hydrophila", Nanomedicine Journal, **1**(3), 198–204 (2014). https://doi.org/10.7508/nmj.2014.03.010

ЗЕЛЕНИЙ СИНТЕЗ НАНОЧАСТИНОК ОКСИДУ МІДІ З ВИКОРИСТАННЯМ РОСЛИНИ MORINGA OLEIFERA ТА ЙОГО ПОДАЛЬША ХАРАКТЕРИЗАЦІЯ ДЛЯ ВИКОРИСТАННЯ У НАКОПИЧУВАЧАХ ЕНЕРГІЇ

Імособоме Л. Іхіоя[a], Едвін У. Оно[a], Агнес К. Нкеле[a,e], Бонавентура К. Абор[a], Б.С.Н. Обітте[a], М. Мааза[b,c,d], Фабіан І. Езема[a,b,c,d]

[a]Факультет фізики та астрономії, Університет Нігерії, Нсукка, 410001, штат Енугу, Нігерія
[b]Африканська мережа нанонаук (NANOAFNET) Національний дослідницький фонд iThemba LABS, 1 Стара Фор-роуд, Сомерсет Вест, Західна Капська провінція, Сомерсет Вест, Південна Африка
[c]Африканська кафедра нанонаук/нанотехнологій ЮНЕСКО-UNISA, Коледж післядипломних досліджень, Університет Південної Африки (UNISA, хребет Макленек, P.O. Box 392, Преторія, Південна Африка
[d]Африканський центр передового досвіду для стійкої енергетики та енергетичного розвитку (ACE-SPED), Університет Нігерії, Нсукка
[e]Факультет фізики, Університет штату Колорадо, Форт-Коллінз, США

Основні моменти дослідження:

• Успішний синтез наночастинок CuO з використанням екстрактів висушеної, дрібно подрібненої Moringa Oleifera як відновника/закриваючого агента

• Зелені синтезовані наночастинки CuO продемонстрували суперємнісну поведінку.

• Спектри відбиття демонструють, що матеріал демонструє низькі властивості відбивання в середньому ультрафіолетовому діапазоні.

• Хороша абсорбція та низькі значення енергії забороненої зони (E_g = 2,5 еВ).

• Потенційне застосування для суперконденсаторів та інших накопичувачів енергії

У цьому дослідженні ми описуємо екологічно чистий синтез оксиду міді (CuO) і його подальшу характеристику для використання в суперконденсаторах. Використовуючи екстракти висушеної, дрібно подрібненої Moringa Oleifera як відновлювача/блокуючого агента, ми створили CuO наночастинки (НЧ). Отримані НЧ потім досліджували за допомогою рентгенівського дифрактометра (XRD), ультрафіолетово-видимої спектроскопії, енергодисперсійної спектроскопії (EDS) і скануючої електронної мікроскопії (SEM). Методи електрохімічного аналізу, такі як циклічна вольтамперометрія (CV) і спектроскопія електрохімічного опору (EIS), були використані для вивчення електрохімічної поведінки електродів на основі CuO. Наступний аналіз визначив, що зелені синтезовані наночастинки CuO демонструють суперємнісну поведінку. Це свідчить про те, що синтезовані наночастинки CuO природним чином заохочуватимуть застосування як суперємнісних електродів, оскільки було виявлено, що поглинання наночастинок змінюється лінійно залежно від концентрації наночастинок, 0,6 моль наночастинок CuO дало найвищий показник поглинання 0,35 при 398 нм. Спектри відбиття демонструють, що матеріал демонструє низькі властивості відбиття в середньому ультрафіолетовому діапазоні. Однак, коли спектр рухається до області видимого світла, коефіцієнт відбиття зростає до максимального значення 16% у короткому ультрафіолетовому діапазоні. Розраховані розміри кристалітів такі: 0,2 моль CuO NP, 0,3 моль CuO NP, 0,4 моль CuO NP, 0,5 моль CuO NP і 0,6 моль CuO NP при 43,14 нм, 43,68 нм, 24,23 нм, 5,70 нм і 12,87 нм, відповідно, де Average D = 25,93 нм є середнім розміром кристалів для всіх зразків. Поява кубічних зерен, які нагадують наностржні з трубчастими отворами, SEM-зображення демонструють, що НЧ CuO можна відрізнити одна від одної, як це видно у на 0,2 моль НЧ CuO.

Ключові слова: *наночастинки CuO; суперконденсатори; накопичувач енергії; Moringa oleifera; циклічна вольтамперометрія*